THEORETICA CHIMICA ACTA

Theoret. Chim. Acta (Berl.) 64, 187–203 (1983)

Electronic states of the [2$_n$]cyclophanes

Jens Spanget-Larsen*

Institut für Organische Chemie der Universität, D-6900 Heidelberg 1,
Federal Republic of Germany

Low energy singlet and triplet states for a series of [2$_n$]cyclophanes are discussed in terms of the results of a simple model calculation. Experimental trends can be explained under the assumption of significant $\sigma - \pi$ interaction involving the saturated bridges. This interaction destabilizes low energy "excimer" states, in contrast to the usual red shift observed for alkylbenzenes. The observed near-constancy of the onset of the absorption spectra can be explained by near-cancelation of through-bond and through-space contributions.

Key words: [2$_n$]Cyclophanes—Excited states of ~—Through-bond and through-space interactions in ~.

1. Introduction

The electronic structure of [2.2]paracyclophane has been a subject of continous research ever since the discovery of the compound in 1949 [1]. In this molecule two benzene rings are kept together by two ethano bridges in a strained face-to-face arrangement with average distance close to 3 Å [2], giving rise to exceptional transannular interactions and unique chemical and physical properties [1–22].

The absorption and emission spectra of [2.2]paracyclophane are strikingly different from those of simple benzene derivatives [5–9, 16–20]. The spectra exhibit anomalous broad bands lacking the typical benzenoid vibrational fine structure, and new transitions are observed which have no counterpart in the benzene spectrum.

* From 01.01.1984, Royal Danish School of Educational Studies, Department of Chemistry, DK-2400 Copenhagen NV, Denmark

The anomalous band shape has been explained by the assumption of large structural rearrangements on excitation or emission [7, 19, 20]. Comparable broadening and loss of fine structure is observed for strained [*n*]paracyclophanes containing a boat-shaped benzene ring [6, 23]. The presence of additional bands can be explained in principle by exciton and charge resonance interactions between the two chromophores. Similar transitions are observed in the emission spectrum from concentrated benzene solutions and have been assigned to excimer fluorescence [24, 25]. However, the assignment of the individual absorption and emission bands for [2.2]paracyclophane has proven a very difficult task, complicated not only by the complexity of the observed overlapping band structures, but also by the divergent results of different theoretical procedures [16, 25–36]. As a consequence, several divergent assignments have been proposed; the range is amply illustrated by comparison of the assignments recommended by Koutecký and Paldus [27], Vala et al. [30], Iwata et al. [16], Duke et al. [33], and Czuchajowsky and Pietrzycki [35].

In this communication we present the results of a comparitive study of a series of [2_n]cyclophanes (Scheme 1), including **2**(1,4) ("paracyclophane"), **3**(1,2,4), **3**(1,3,5), **4**(1,2,3,4), **4**(1,2,3,5), **4**(1,2,4,5), **5** and **6** ("superphane"). For simplicity we use the labeling introduced in Ref. [21], i.e., [2.2](1,4)cyclophane = **2**(1,4), etc. In these compounds the two benzene rings can be considered to be approximately parallel and eclipsed, with mean inter-ring distances varying from 3.00 Å for **2**(1,4) [2] to 2.63 Å for **6** [37] (Table 1). These compounds form an ideal series for the application of empirical correlation procedures, as demonstrated by the treatment of the photoelectron (PE) data by Heilbronner et al. [21]. In the ensuing study, we apply this powerful technique in an investigation of excited states for these species.

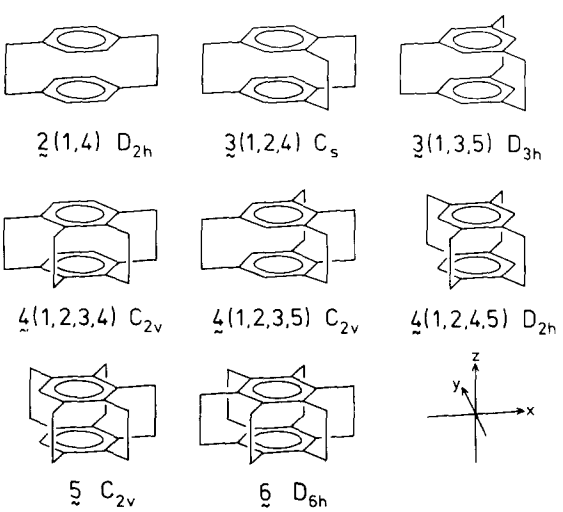

Scheme 1

Table 1. Mean inter-deck distances D [2, 37], first ionization energies I_1 [21], and transannular core integrals $\beta_{\mu\mu'}$ according to Eq. (2.3)

Compound	D/Å	I_1/eV	$\beta_{\mu\mu'}$/eV	$\beta_{\mu\mu'}$/cm^{-1}
2(1,4)	3.00	8.10	−0.63	−5080
3(1,2.4)		8.0	−0.70	−5650
3(1,3,5)	2.79	7.70	−0.91	−7340
4(1,2,3,4)	2.93	7.9	−0.77	−6210
4(1,2,3,5)	2.74	7.75	−0.88	−7100
4(1,2,4,5)	2.78	7.67	−0.93	−7500
5	2.70	7.67	−0.93	−7500
6	2.63	7.55	−1.02	−8230

In particular, we wish to address the following questions: Why is the onset of the absorption spectrum almost constant through the series **2**(1,4)−**6**, in spite of a considerable lowering of the inter-deck distance and increased alkyl substitution? Both effects would intuitively be expected to lead to a marked red shift. Can a transition corresponding to the benzene ^1L_b band be identified in the spectra of [2$_n$]cyclophanes? Why does the absorption spectrum of **3**(1,3,5) look so different? What is the nature of the two low-lying triplet states?

2. Theoretical procedure

Theoretical approaches to the excited states of cyclophanes frequently neglect the influence of the saturated bridges, considering the [2$_n$]cyclophanes as model compounds for a face-to-face benzene dimer. However, as previously pointed out by Gleiter [31] and subsequently verified by PE spectroscopy [14, 15, 21, 22], σ-π interactions involving the bridging groups have a profound impact on the electronic structure. In the following is described a simple model based on standard Pariser–Parr–Pople (PPP) theory [38], but with inclusion of transannular through-bond and through-space effects.

The benzene rings are considered as eclipsed regular hexagons with an inter-deck distance of 2.8 Å; this distance is intermediate between the experimental values for **2**(1,4) and **6** (Table 1) and is kept constant for all compounds. The highest occupied σ orbital of a bridging ethano group [15, 21, 31] is represented as the in-phase combination of two pseudo methylene π orbitals (the out-of-phase combination is excluded from the basis set). The resulting basis set and choice of phases is indicated in Fig. 1.

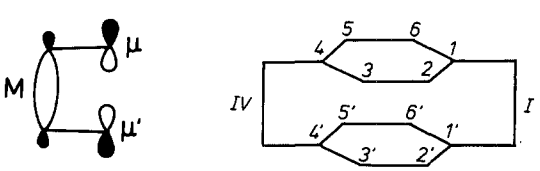

Fig. 1. Basis orbitals for the PPP calculations, with definition of phases for the benzene π atomic orbitals (μ, μ') and the semi-localized ethano σ orbital (M). Numbering of the resulting basis orbitals is indicated for **2**(1,4)

For the benzene π atomic orbitals the effective ionization energy is taken as 9.8 eV and the intra-ring two-centre core integrals as $\beta_{\mu\nu} = -2.318$ eV for neighbours and zero otherwise. The intra-deck repulsion integrals $\gamma_{\mu\nu}$ are computed according to the Mataga–Nishimoto formula [39] with $\gamma_{\mu\mu} = 10.84$ eV, thereby ensuring the correct spacing in energy of the benzene ^1L_b and ^1L_a states in the mono-excited configuration interaction (CI) picture. The orbital energy of the semi-localized σ orbital is taken as -14.0 eV [15, 21, 31] and the $\sigma-\pi$ core integrals as $\beta_{\mu M} = \beta_{\mu' M} = -2.1$ eV. This value is consistent with the value -2.4 eV adopted by Heilbronner et al. [15, 21] for the corresponding Hückel (HMO) "resonance integral", since

$$\beta_{\mu\nu}^{\mathrm{HMO}} \approx F_{\mu\nu}^{\mathrm{PPP}} = \beta_{\mu\nu} - p_{\mu\nu}\gamma_{\mu\nu}/2. \tag{2.1}$$

The inter-deck core integrals $\beta_{\mu\nu'}$ are treated according to the intersubsystem tight-binding approximation recommended by Vogler [36], i.e. only "first neighbour" terms $\beta_{\mu\mu'}$, corresponding to the atomic orbitals μ, μ' directly above each other, are retained. As shown by Vogler [36], an appropriate treatment of overlap effects (using Löwdin orthogonalized atomic orbitals) leads to negligibly small values for inter-deck core integrals other than $\beta_{\mu\mu'}$. This is an important simplification which preserves the alternant pairing symmetry for the D_{6h} benzene dimer in the PPP model [42, 43]. Moreover, the core integral τ between any two equivalent normalized benzene π orbitals localized on different rings reduces in the model to the diatomic integral $\beta_{\mu\mu'}$, i.e. $\tau = \beta_{\mu\mu'}$. Within the framework of Hückel theory, Heilbronner et al. [21] calibrated the value of the corresponding "resonance integral" τ^{HMO} by means of the relation

$$\tau^{\mathrm{HMO}} = -9.0 + I_1 \tag{2.2}$$

where -9.0 eV is the estimated basis orbital energy for the benzene $e_{1g}(\pi)$ level and I_1 is the observed first ionization energy for the [2$_n$]cyclophane in question. Unfortunately, the values derived according to Eq. (2.2) cannot be equated directly to PPP τ or $\beta_{\mu\mu'}$ terms, partly because of the inequivalence of HMO and PPP parameters indicated in Eq. (2.1), but particularly because the self-consistent-field PPP model accounts explicitly for certain inductive effects on the diagonal matrix elements, effects which in the HMO treatment [21] are considered implicitly through the empirical calibration of off-diagonal matrix elements in Eq. (2.2). However, rather than generate a completely new set of parameter values, we have assumed the simple proportionality relation

$$\beta_{\mu\mu'} = c \cdot \tau^{\mathrm{HMO}} \tag{2.3}$$

where c is a numerical constant which should be less than unity (particularly because of the inductive effect absorbed in τ^{HMO}). The constant c is set equal to 0.7, which leads to good agreement between calculated orbital diagrams and a number of observed trends (Sect. 3). The resulting $\beta_{\mu\mu'}$ values range from -0.63 eV for **2**(1,4) to -1.02 eV for **6** (Table 1). As discussed in detail by Heilbronner et al. [21], the variation essentially reflects the dependence on the actual mean inter-deck distance.

Regarding the inter-deck electron repulsion integrals $\gamma_{\mu\nu'}$, it is likely that application of the Mataga–Nishimoto approximation for intra- as well as inter-deck terms would underestimate the relative magnitude of the latter, because of the different mode of overlap and the smaller correlation energy involved [40]. For these terms we apply the Dewar–Sabelli–Ohno–Klopman approximation [41]. The $\gamma_{\mu\nu'}$ values are calculated for a fixed inter-deck distance equal to 2.8 Å (see above); results of trial calculations indicate that the dependence on the actual distance is small and affects insignificantly the trends of the calculated transitions.

Singlet and triplet states are generated by CI between mono-excited configurations involving excitations from the six highest occupied to the six lowest unoccupied MOs. In the absence of $\sigma-\pi$ interaction, i.e. for $\beta_{\mu M}=0$, the model contains the alternant pairing symmetry [42], implying that states can be characterized as "plus" or "minus" [43]. For $\beta_{\mu M}=-2.1$ eV, the pairing symmetry is perturbed but still significant. The shifts of the calculated transitions for the series **2**(1,4)–**6** depend solely on two factors: variation in inter-deck through-space interaction as reflected by the parameters $\beta_{\mu\mu'}$, and the variation in number and position of the bridging through-bond relay orbitals, which also define the spatial symmetry of the system.

3. Orbital energies

The "frontier" orbitals for **2**(1,4) are indicated in Fig. 2, and the correlation of calculated orbital energies for the series is shown in Fig. 3. The labeling s_+, a_-, etc., is defined in Fig. 2; a survey of the orbital symmetry properties for the [2$_n$]cyclophanes can be found in Ref. [21]. For reasons of symmetry, the minus-combinations s_-, a_-, $s_\pm^*$, $a_\pm^*$ are not affected by through-bond interaction via the ethano orbitals M and stay pairwise near-degenerate (they may, however, interact with other orbitals, e.g. σ^* orbitals, not considered in the model, but this interaction seems to be relatively insignificant [31]). The calculated energy is thus an approximate measure of the transannular through-space interaction represented by the empirical parameters $\beta_{\mu\mu'}$; this, of course, is the theoretical foundation for Eqs. (2.2) and (2.3). In contrast, the plus-combinations s_+, a_+, $s_\mp^*$, $a_\mp^*$ are generally destabilized and split by the through-bond interaction, $s_\mp^*$ and $a_\mp^*$ less strongly than s_+ and a_+ because of the larger distance in energy to the σ relay orbitals. **2**(1,4) is unique in that only s_+ and $s_\mp^*$ are affected by through-bond interaction, leading to particularly large splittings in this case.

Within a simple Koopmans' picture [44], the ordering and spacing of the occupied levels is consistent with the trends of the PE data indicated in Fig. 4, and with the electronic absorption spectrum of the radical cation **2**(1,4)$^+$ [12, 21]. Similarly, the virtual orbital diagram is consistent with the electron spin resonance and electronic absorption data for the radical anion **2**(1,4)$^-$ [10, 11, 30, 45]. For example, the measured hyperfine constants for **2**(1,4)$^-$ indicate that $b_{1g}(a_\mp^*)$ and not $a_g(s_\mp^*)$ takes up the unpaired electron [11]. Gerson and Martin [11] and Duke et al. [33] interprete this finding in terms of inductive effects, destabilizing $a_g(s_\mp^*)$ more strongly than $b_{1g}(a_\mp^*)$. However, according to the results of the

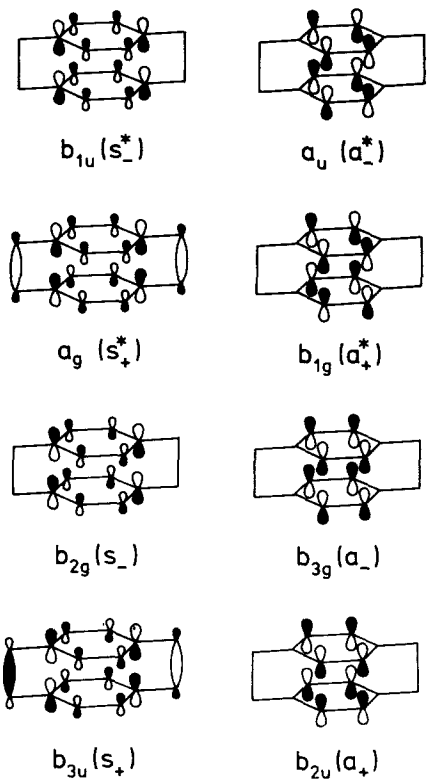

Fig. 2. Schematical representation of the "frontier" orbitals of **2**(1,4), derived by through-space and through-bond interaction of benzene $e_{1g}(\pi)$ and $e_{2u}(\pi^*)$ type orbitals

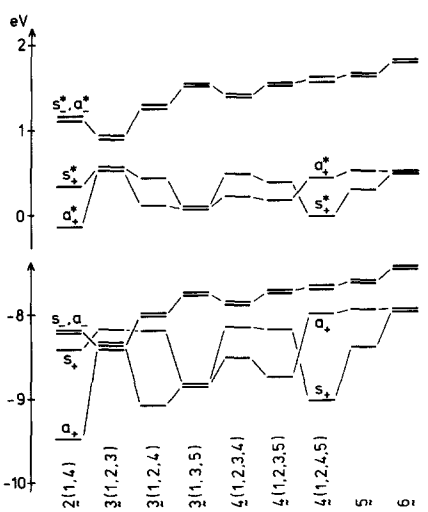

Fig. 3. Correlation of calculated "frontier" orbital energies for **2**(1,4)–**6** (incl. also "clam-shaped" **3**(1,2,3) for comparison with the PE data in Fig. 4)

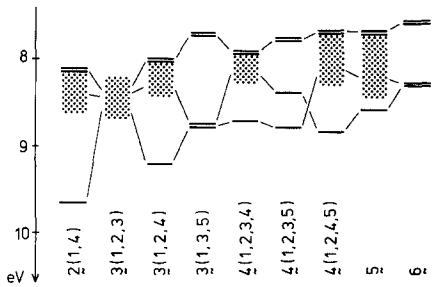

Fig. 4. Correlation of observed ionization energies for **2**(1,4)–**6** [21]

calculation, through-bond effects are more significant for the splitting in energy of these orbitals. The absorption spectrum of $\mathbf{2}(1,4)^{\mp}$ features an intense band with onset at 1000 nm (1.2 eV) and maximum at 760 nm (1.6 eV) [10]. This band can be assigned to the z-polarized charge resonance transition $^2B_{1g} \rightarrow {}^2A_u$, corresponding to the promotion of an electron from $b_{1g}(a_+^*)$ to $a_u(a_-^*)$. Since both orbitals are unaffected by through-bond effects, the observed transition energy (and intensity) is fairly direct evidence for the transannular through-space interaction in $\mathbf{2}(1,4)^{\mp}$; the predicted promotion energy is essentially equal to $|2\beta_{\mu\mu'}| = 1.3$ eV.

4. Electronic states

The states can be classified according to their transformation properties with respect to the inter-deck plane of symmetry present for the assumed idealized structures; in the case of **3**(1,2,4) this is the only symmetry element present. Considering the sixteen states which can be derived by promotion of an electron from the occupied orbitals s_+, a_+, s_-, a_- to the unoccupied orbitals s_+^*, a_+^*, s_-^*, a_-^*, eight of these transform according to the irreducible representation A' and the remaining eight according to the irreducible representation A'' of the C_s subgroup. A survey of symmetry labels is given in Table 2.

Table 2. Survey of symmetry labels for low-lying excited singlet states, including the first four members of the $^1A''$ and the first six members of the $^1A'$ manifold

Symmetry[a]	Compd.	$^1A''$	$^1A'$
D_{6h}	**6**	$^1B_{1g}^- \; ^1B_{2g}^+ \quad ^1E_{1g}^+$	$^1B_{2u}^- \; ^1B_{1u}^- \quad ^1E_{1u}^- \quad ^1B_{2u}^+ \; ^1B_{1u}^+$
D_{3h}	**3**(1,3,5)	$^1A_1''^- \; ^1A_2''^+ \quad ^1E''^+$	$^1A_2'^- \; ^1A_1'^- \quad ^1E'^- \quad ^1A_2'^+ \; ^1A_1'^+$
D_{2h}	**2**(1,4)	$^1B_{3g}^- \; ^1B_{2g}^+ \; ^1B_{3g}^+ \; ^1B_{2g}^+$	$^1B_{2u}^- \; ^1B_{3u}^- \; ^1B_{2u}^- \; ^1B_{3u}^- \; ^1B_{2u}^+ \; ^1B_{3u}^+$
	4(1,2,4,5)		
C_{2v}	**4**(1,2,3,4)	$^1B_2^- \; ^1A_2^+ \; ^1B_2^+ \; ^1A_2^+$	$^1A_1^- \; ^1B_1^- \; ^1A_1^- \; ^1B_1^- \; ^1A_1^+ \; ^1B_1^+$
C_{2v}	**4**(1,2,3,5)	$^1A_2^- \; ^1B_2^+ \; ^1A_2^+ \; ^1B_2^+$	$^1B_1^- \; ^1A_1^- \; ^1B_1^- \; ^1A_1^- \; ^1B_1^+ \; ^1A_1^+$
	5		
C_s	**3**(1,2,4)	$^1A''^- \; ^1A''^+ \; ^1A''^+ \; ^1A''^+$	$^1A'^- \; ^1A'^- \; ^1A'^- \; ^1A'^- \; ^1A'^+ \; ^1A'^+$

[a] Labeling of axes is given in Scheme 1, except for the C_{2v} species where the z axis and the z, x plane are taken as the C_2 axis and the inter-deck plane of symmetry.

The eight A'' states can be divided into a group of four states at low energy, corresponding to promotion from s_-, a_- to s_+^*, a_+^*, and another group of four states at higher energies, corresponding to promotion from s_+, a_+ to s_-^*, a_-^*. The four low-energy states correspond to excimer states, characterized by positive transannular bond orders $p_{\mu\mu'}$. The A'' states are "gerade" with respect to the inversion symmetry present for **2**(1,4), **4**(1,2,4,5) and **6**. One-photon transitions from the ground state are either z-polarized or symmetry forbidden within the full point group.

The eight A' states correspond to promotion from s_-, a_- to s_-^*, a_-^* and from s_+, a_+ to s_+^*, a_+^*. They are affected by essentially first order CI and cover a large region of energy. They are 'ungerade' with respect to inversion symmetry, when present, and one-photon transitons from the ground state are either polarized in the x, y-plane, or electronically forbidden.

4.1. Excited singlet states

Calculated transitions are indicated in Figs. 5 and 6. The four excimer $^1A''$ states are predicted in the 30–40 000 cm^{-1} region. The lowest two excited singlet states are predicted to be of this class. The high-energy $^1A''$ states are placed above 46 000 cm^{-1}. The $^1A''$ states occur from 35 000 cm^{-1} and above; six of them are predicted below 50 000 cm^{-1}. The lowest $^1A'$ state is well separated from those at higher energies and is generally predicted as the third excited singlet. This

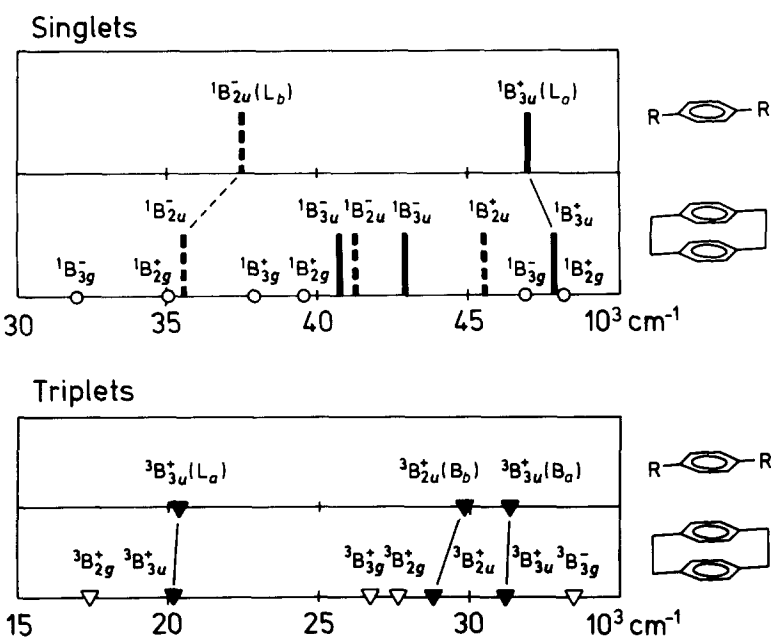

Fig. 5. Calculated singlet and triplet transitions for **2**(1,4) and a simple D_{2h} p-dialkylbenzene; the calculation for the latter species corresponds to that for **2**(1,4), except for the omission of one benzene ring. For explanation of symbolism, see legend to Fig. 6

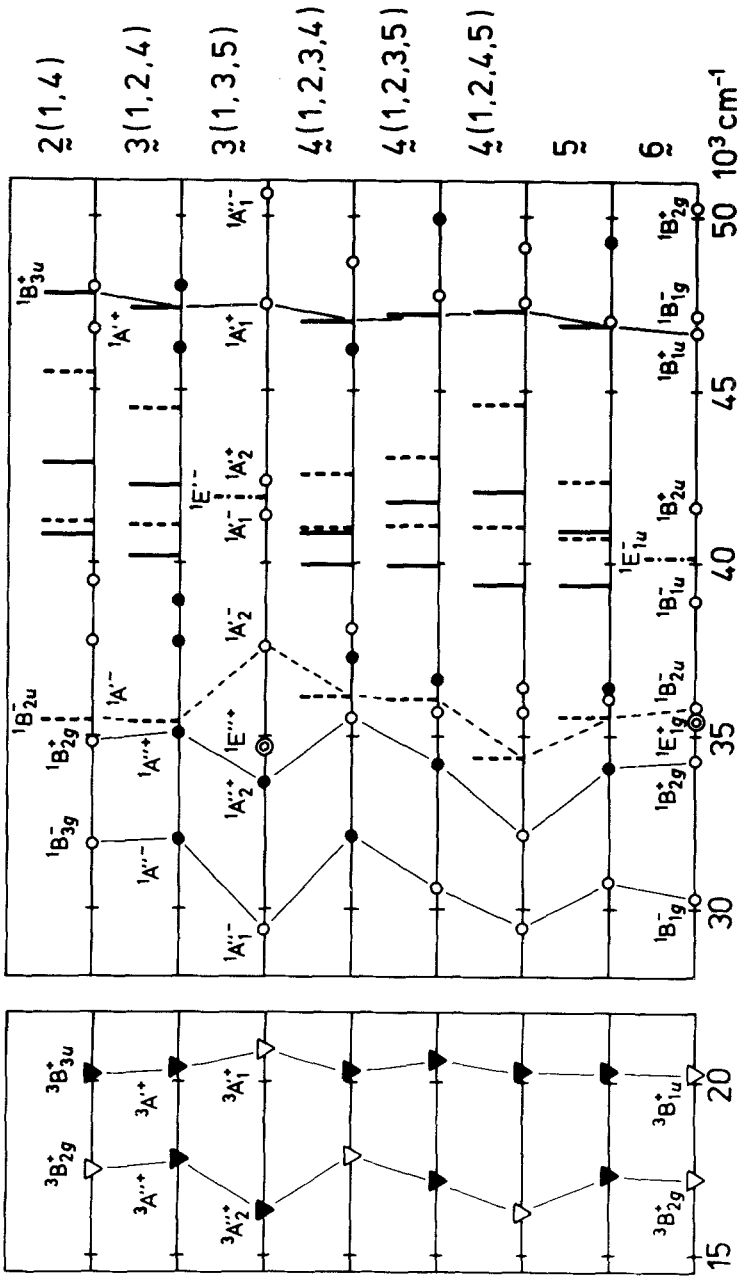

Fig. 6. Calculated transitions for **2**(1,4)–**6**. x and y polarized transitions are indicated by full and broken bars, respectively (indication of x,y-polarization directions for **3**(1,2,4) is approximate). Forbidden and z-polarized transitions are indicated by white and black circles, respectively. Triplet states are indicated by triangles; white (black) triangles indicate that transition to the ground state is forbidden (allowed) by the spatial symmetry. Labeling of axes is given in Scheme 1

state can be correlated with the ^1L_b state of an alkyl substituted benzene but is predicted at lower energy (e.g., Fig. 5).

The results in Fig. 5 (top) are consistent with the general structure of the observed absorption spectrum of **2**(1,4) and with the shifts observed relative to the spectrum of a "normal" 1,4-dialkylbenzene [5–7, 16–18]. The 30–40 000 cm^{-1} region is characterized by weak one-photon and strong two-photon absorption, while the absorption in the 40–50 000 cm^{-1} region is medium intense in one-photon and weak in two-photon spectroscopy. These observations are consistent with the predicted distributions of '*g*' and '*u*' states. The polarized one-photon crystal spectrum [7, 16, 17] indicates overlapping of differently polarized contributions throughout the investigated spectral range. Assignment of the diffuse absorption in the 40–50 000 cm^{-1} region to individual transitions is difficult, particularly in view of the expected vibronic contributions. The number of states predicted in this region is obviously sufficient to account for the observed absorption. Hence, we refrain from further discussion of this spectral region and concentrate on the possible assignment of the more interesting low-energy transitions.

4.1.1. The lowest excited $^1A''$ *state.* The lowest excited singlet state of the [2_n]cyclophanes is generally considered to be of excimer character, corresponding to the first member of the $^1A''$ manifold. One would expect the transition to an excimer state to be extremely sensitive to the inter-deck separation [27, 30]. However, the onset of the absorption spectra of **2**(1,4)–**6** is remarkably constant: within ±1000 cm^{-1}, the first "vertical feature" is located at 33 000 cm^{-1}. The positions indicated in Fig. 7 (right) correspond to the very first weak band in the solution spectrum at room temperature, typically a structureless maximum or shoulder with $\varepsilon \approx 200$, taken from the literature [5, 6, 33, 46–52] or re-measured in cyclohexane by the author (**5** and **6**). Due to the diffuseness of the bands and the influence of different solvents, the indicated positions are only approximate. However, the practically identical transition energies for **2**(1,4) and **6**, in spite of a difference in mean inter-deck distance by almost 0.4 Å, are remarkable and seem to speak against the assignment of an excimer state.

Fig. 7 also indicates the calculated $S_0 \rightarrow S_1$ transition energies for the series. In the absence of through-bond effects, i.e. for the assumption of $\beta_{\mu M} = 0$, the results of the model reduce to those for a D_{6h} benzene dimer. In this case, the calculated $S_0 \rightarrow S_1$ transition energy is essentially equal to a constant term minus twice the transannular $|\beta_{\mu\mu'}|$ parameter:

$$E(S_0 \rightarrow S_1) \approx 40\,600\ cm^{-1} - |2\beta_{\mu\mu'}| \tag{3.1}$$

Hence, the transition is shifted towards *lower* energies through the series **2**(1,4)–**6**, from 30 400 to 24 200 cm^{-1} (Fig. 7, broken line), reflecting the dependence of through-space interaction on the actual inter-deck separation. This result is in poor agreement with the near-constancy of the experimental energies. However, inclusion of through-bond contributions is seen to improve the agreement drastically. This can be explained by the fact that, for reasons of symmetry, through-bond interaction destabilizes the virtual orbitals s_+^*, a_+^* but leaves the occupied

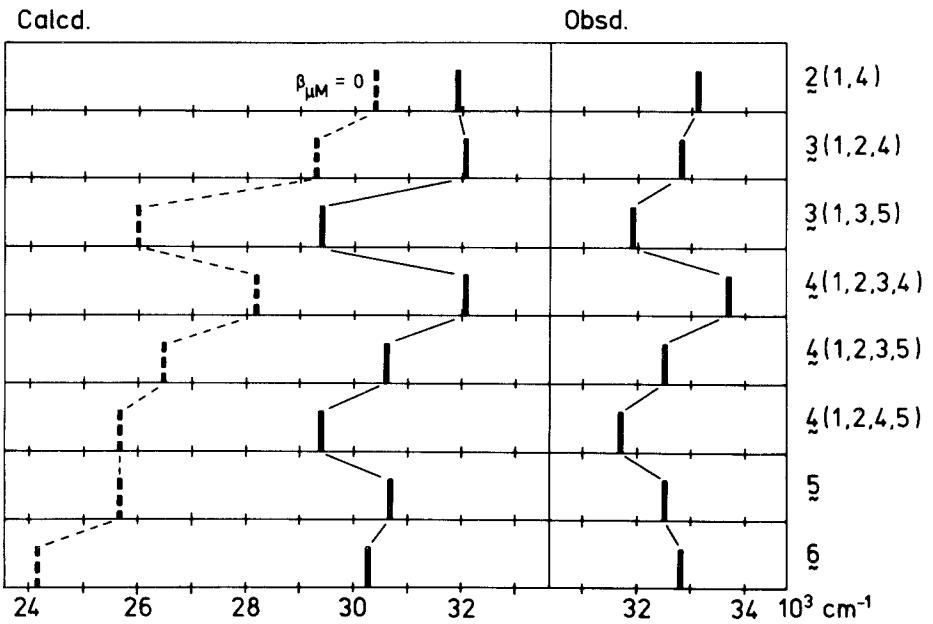

Fig. 7. (left) Calculated transitions to the lowest $^1A''$ state, with and without consideration of through-bond effects (full and broken bars, respectively). **(right)** Observed onset of the UV absorption spectra [5, 6, 33, 46–52]

orbitals s_-, a_- unaffected, thereby shifting low-energy A'' states towards *higher* energies. This shift is roughly proportional to the number of alkyl bridges and tends to cancel with the shift caused by the increasing through-space interaction. The final results of the calculation, representing a super-position of through-space and through-bond effects, are indicated in Fig. 7 and can be written approximately as

$$E(S_0 \rightarrow S_1) \approx 40\,600\ \text{cm}^{-1} - |2\beta_{\mu\mu'}| + n \cdot k \tag{3.2}$$

where n is the number of bridging groups and k is close to 1000 cm^{-1}. In view of the simplicity of the model, the predicted energies are pleasingly consistent with the experimental evidence. A number of trends, such as the relatively low energy for **3**(1,3,5) and **4**(1,2,4,5), and the relatively high energy for **4**(1,2,3,4), seem well reproduced. Eq. (3.2) thus offers a simple rationalization not only of the near-constancy of the observed $S_0 \rightarrow S_1$ transition energies, but also of the magnitude and sign of the more significant of the individual shifts.

4.1.2. The lowest excited $^1A'$ state. In the absorption spectrum of **2**(1,4), the absolute maximum of the low-energy band is located close to 35 000 cm^{-1} [5, 6, 33]. Previous investigations have, with notable exceptions (e.g., Refs. [16–18]), associated this maximum with transition to the $^1B_{2u}^-$ state; this is the first excited $^1A'$ state of **2**(1,4) and is closely related to the ^1L_b state of a *p*-disubstituted benzene (Fig. 5). In Fig. 8 (right) is indicated the position of this maximum

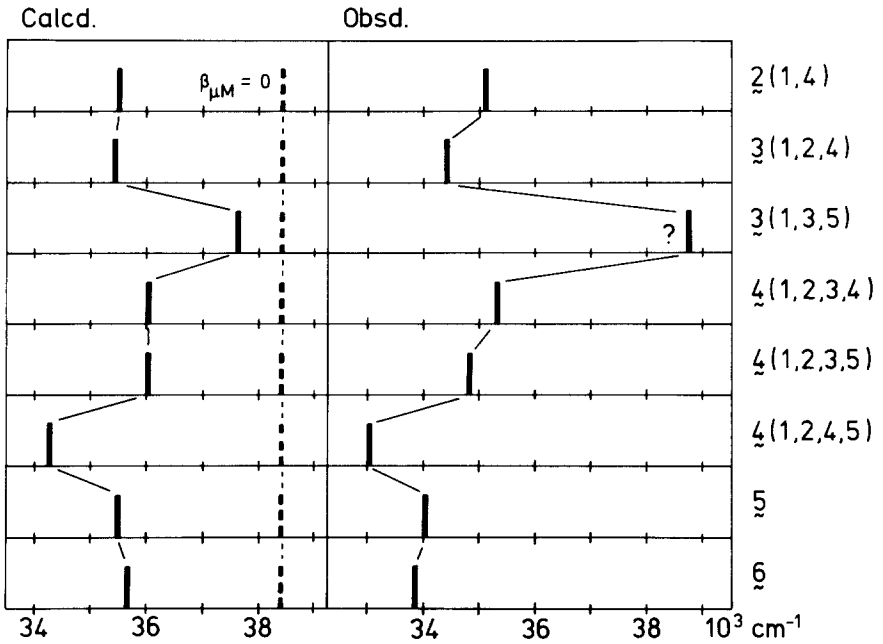

Fig. 8. (left) Calculated transitions to the lowest excited $^1A'$ state, with and without consideration of through-bond effects (full and broken bars, respectively). **(right)** Observed absorption maxima for the 30–40 000 cm^{-1} absorption band [5, 6, 33, 46–52]

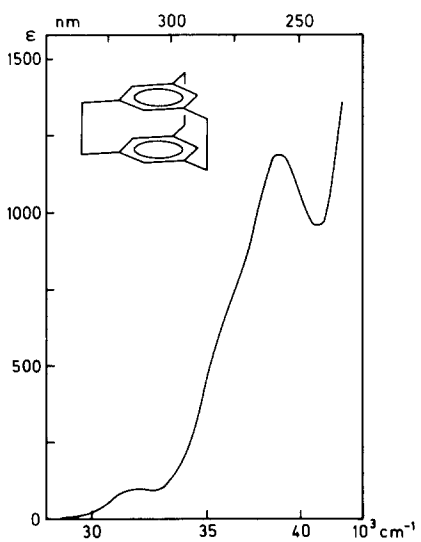

Fig. 9. Near-UV absorption spectrum for **3**(1,3,5) in hexane. Reproduced with permission from the doctoral thesis of R. A. Hollins [47]

($\varepsilon \approx 400$) as a function of the substitution pattern; it is generally located 1–2000 cm^{-1} above the first weak feature discussed in the previous paragraph. However, the absorption spectrum of **3**(1,3,5) shown in Fig. 9 is different from those of other [2$_n$]cyclophanes. It features a well defined and relatively intense maximum at 38 800 cm^{-1} which is not easily correlated with transitions of the

remaining compounds. Hence, there seems to be something particular about the electronic structure of **3**(1,3,5) which gives rise to a deviating absorption spectrum.

As previously mentioned, the results of the model correspond to those for a D_{6h} benzene dimer when $\beta_{\mu M}$ is set equal to zero. For reasons of symmetry, a constant energy is then obtained for the lowest excited $^1A'$ state ($^1B_{2u}^-$ in D_{6h}) independent of the through-space interaction, namely identically the same energy as predicted for the $^1B_{2u}^-(L_b)$ state of benzene, 38 400 cm^{-1} (exciton and charge resonance interactions are forbidden, either by the spatial or by the alternant pairing symmetry). Introduction of through-bond contributions shifts this state towards lower energies, as anticipated by Gleiter [31]. This is because of larger destabilization of the occupied s_+, a_+ than of the unoccupied s_+^*, a_+^* orbitals, thereby stabilizing s_+, $a_+ \rightarrow s_+^*$, a_+^* configurations which become the leading contributions to the lowest excited $^1A'$ states. However, the through-bond effect is sensitive to details of the MO level diagram and to the extent of CI, depending on the perturbation of the spatial and the pairing symmetry by the bridging groups. The through-bond effect is not proportional to the number of alkyl groups and a simple expression, similar to Eq. (3.2), does not apply to the energy of the lowest excited $^1A'$ state; the predicted energies are indicated in Fig. 8 (left). It is seen that very similar effects are obtained, except for the prediction of a relatively high and a relatively low transition energy for **3**(1,3,5) and **4**(1,2,4,5), respectively. This trend can be explained by consideration of the difference in energy between the lowest unoccupied and the third highest occupied MOs (Fig. 3).

Within the limits of significance, the predicted trend is in fairly good agreement with the shifts of the observed maxima. This result seems to support the assumption that transition to the lowest member of the excited $^1A'$ manifold occurs in the low-energy region, probably associated with the absolute band maximum. The results do not support the assignment in Refs. [16–18] of a shoulder at 41 000 cm^{-1} in the solution spectrum **2**(1,4) to this state ($^1B_{2u}(\alpha)$ in the nomenclature of these authors). This assignment implies that the benzene ^1L_b or α transition is blue shifted in **2**(1,4), which is incompatible with the theoretical results and with the red shifts observed for related alkylbenzenes and [n]cyclophanes [5, 6, 23, 53].

According to the results of the model calculation, the puzzling spectrum of **3**(1,3,5) can be explained in part by the prediction of an exceptionally large distance in energy between the lowest excited $^1A''$ and $^1A'$ states ($^1A_1''^-$ and $^1A_2'^-$ in D_{3h}; Fig. 6). This may explain the separation of the first and the second maximum by almost 7000 cm^{-1}. The prediction can be understood by noticing the particularly large energy separation of the s_+, a_+ and s_-, a_- orbitals for **3**(1,3,5) (Fig. 3). Hence, the calculated electronic structure is rather dominated by the through-space contribution, a result of the symmetry restriction of the through-bond effect and of the relatively small inter-deck distance by the presence of only three bridging groups.

However, tentative assignment of the 38 800 cm^{-1} band of **3**(1,3,5) to the $^1A_2'^-$ state does not explain the increased intensity ($\varepsilon = 1200$). A similar hyperchromic shift is observed for the 33 000 cm^{-1} band of **4**(1,2,4,5) ($\varepsilon = 1050$) [50]; but this

shift is expected from the corresponding hyperchromic shift of the $^1L_b^-$ band of 1,2,4,5-tetramethylbenzene [54] and is consistent with the calculation of a particularly large oscillator strength for **4**(1,2,4,5) ($f = 0.07$). In contrast, transition to the $^1A_2'^-$ state of **3**(1,3,5) is forbidden by symmetry. The observed intensity can probably be explained by contributions from allowed transitions (i.e., to the $^1A_2''^+$ state), by vibronic interactions, and by a deviation from the assumed D_{3h} symmetry in ground and/or excited states. A torsional dimer distortion to a structure of D_3 symmetry, similar to the distortion discussed for **2**(1,4) [2, 7, 20], changes A_2' to A_2 and transition from the ground state gains z-polarized intensity. Note that the corresponding distortion of "superphane" (**6**) from D_{6h} to D_6, thereby changing B_{2u} to B_2, does not change $^1B_{2u}^-$ into an optically allowed state.

4.2. Triplet states

The phosphorescence spectrum of **2**(1,4) has been investigated by several authors [8, 9, 19, 20]. Relative to the spectrum of *p*-xylene [55], the onset of the phosphorescence band of **2**(1,4) is red shifted by almost 4000 cm^{-1}; at the same time, the band is strongly broadened, with a weak 0–0 component at 24 600 cm^{-1} and maximum at 21 000 cm^{-1} in the low-temperature crystal spectrum [19, 20]. Moreover, from an investigation of the zero field splitting parameters, Melzer et al. [19] were able to identify *two* radiating near-degenerate triplet states for **2**(1,4) with lifetimes 5 *s* for T_1 and 0.6 *s* for T_2. By reference to the two lowest excited singlets, these states were tentatively assigned as $^3B_{3g}$ and $^3B_{2g}$ ($^3B_{2g}$ and $^3B_{3g}$, respectively, in the coordinate system of Ref. [19]).

The calculated triplet states for **2**(1,4) are indicated in Fig. 5. The results are reasonably consistent with the experimental evidence, but suggest an alternative assignment of the two low-energy triplets, namely $^3B_{2g}^+$ and $^3B_{3u}^+$. The $^3B_{2g}^+$ state corresponds to the second excited singlet and is of excimer character, the $^3B_{3u}^+$ state correlates with the $^3B_{3u}^+(L_a)$ state of a *p*-dialkylbenzene. It is unlikely that either T_1 or T_2 are related to the lowest excited singlet state, $^1B_{3g}^-$, as suggested by Melzer et al. [19], since this is a "minus" state, indicating small singlet-triplet splitting [43]. In fact, the $^3B_{3g}^-$ state is calculated as the seventh triplet. However, the assignment of $^3B_{2g}^+$ and $^3B_{3u}^+$ is consistent with the relative life-times, 5 s and 0.6 s, respectively, since transition from $^3B_{2g}^+$ is spin and space forbidden whereas transition from $^3B_{3u}^+$ is only spin forbidden (this consideration assumes that the ratio of the observed lifetimes is not strongly affected by non-radiative processes). Furthermore, different equilibrium structures are expected for these states, since the $^3B_{2g}^+$ excimer state is bonding and the $^3B_{3u}^+$ state essentially non-bonding with respect to inter-deck interactions. This is nicely consistent with the assumptions of Melzer et al. [19].

In Fig. 6 are indicated the calculated shifts of the two lowest triplets, $^3A''^+$ and $^3A'^+$ in the C_s point group, for the series **2**(1,4)–**6**. The shifts of $^3A''^+$ are similar to those of the closely related $^1A''^+$ state, reflecting the excimer nature of both

states. The predicted energy of the $^3A'^+$ state is constant within a few hundred cm^{-1}. A similar result is obtained for the corresponding singlet state $^1A'^+$ predicted between 47 000 and 48 000 cm^{-1} for all compounds. A relatively large splitting of $^3A_2''^+$ and $^3A_1'^+$ is predicted for **3**(1,3,5); moreover, if spatial symmetry differences are responsible for the relative decay probabilities, $T_1(^3A_2''^+)$ should be shortlived relative to $T_2(^3A_1'^+)$. It is thus possible that not only absorption but also emission data for **3**(1,3,5) deviate from those of typical [2$_n$]cyclophanes.

5. Concluding remarks

Before concluding this communication, it is necessary to emphasize the qualitative nature of the presented results. The theoretical model is based on an extension of standard π electron theory to incorporate interaction with σ orbitals [56] but is severely truncated with respect to orbital basis and CI expansion and neglects effects due to distortion of the benzene rings and deviation from the assumed idealized symmetry. Moreover, the observed spectra indicate the importance of vibronic interactions and structural rearrangements on excitation, contributions which are neglected in the model. Finally, due to the high density of states, the spectral features discussed are probably the result of several overlapping transitions, which complicates precise conclusions. One should certainly be careful not to underrate the complexity of the electronic structure of these compounds.

Nevertheless, we find that the simple model yields a pleasing insight into the main effects that are responsible for the long wave absorption of [2$_n$]cyclophanes. Hyperconjugative interactions with the bridging groups shift transitions to low-lying "excimer" states towards *higher* energies, in contrast to the usual red shift observed on alkylation of benzene [54]. This can be explained by through-bond coupling of π^* orbitals and is another manifestation of the particular symmetry conditions prevailing in [2$_n$]cyclophanes [21]. Low-lying "non-excimer" states are as a rule shifted towards *lower* energies by the through-bond effect. As a consequence, the predicted ordering of low-energy states may be sensitive to calculational details. On the basis of the calculated results, suggestions can be made concerning the origin of the apparently deviating spectral properties of **3**(1,3,5); further conclusions probably require detailed experimental investigations.

Acknowledgments. The author is indebted to Professor Dr. R. Gleiter for generous support of this investigation. Kind gifts of samples and spectra from Professor Dr. V. Boekelheide and Professor Dr. H. Hopf are gratefully acknowledged. Special thanks are due to Professor Dr. E. Heilbronner and Dr. H. Vogler for critical reading of the manuscript.

References

1. Brown, C. J., Farthing, A. C.: Nature (London) **164**, 915 (1949)
2. Brown, C. J.: J. Chem. Soc., 3265 (1953); Lonsdale, K., Milledge, J. J., Rao, K. V. K.: Proc.

Roy. Soc. **A255**, 82 (1960); Hope, H., Bernstein, J., Trueblood, K. N.: Acta Cryst. **B28**, 1733 (1972)
3. Cram, D. J., Cram, J. M.: Acc. Chem. Res. **4**, 204 (1971); Vögtle, F., Neumann, P.: Top. Curr. Chem. **48**, 67 (1974); Vögtle, F., Hohner, G.: Top. Curr. Chem. **74**, 1 (1978)
4. Boekelheide, V.: Acc. Chem. Res. **13**, 65 (1980); Kleinschroth, J., Hopf, H.: Angew. Chem. **94**, 485 (1982); Angew. Chem. Int. Ed. Engl. **21**, 469 (1982)
5. Cram, D. J., Steinberg, H.: J. Am. Chem. Soc. **73**, 5691 (1951)
6. Cram, D. J., Allinger, N. L., Steinberg, H.: J. Am. Chem. Soc. **76**, 6132 (1954)
7. Ron, A., Schnepp, O.: J. Chem. Phys. **37**, 2540 (1962); **44**, 19 (1966)
8. El-Sayed, M. A.: Nature (London) **197**, 481 (1963)
9. Helgeson, R. C., Cram, D. J.: J. Am. Chem. Soc. **88**, 509 (1965)
10. Ishitani, A., Nagakura, S.: Mol. Phys. **12**, 1 (1967)
11. Gerson, F., Martin, W. B.: J. Am. Chem. Soc. **91**, 1883 (1969)
12. Badger, B., Brocklehurst, B.: Trans. Faraday Soc. **65**, 2582 (1969); **66**, 2939 (1970)
13. Pignataro, S., Mancini, V., Ridyard, J. N. A., Lempka, H. J.: Chem. Commun. 142 (1971)
14. Boschi, R., Schmidt, W.: Angew. Chem. **83**, 408 (1973); Angew. Chem. Int. Ed. Engl. **12**, 402 (1973)
15. Heilbronner, E., Maier, J. P.: Helv. Chim. Acta **57**, 151 (1974)
16. Iwata, S., Fuke, K., Sasaki, M., Nagakura, S., Otsubo, T., Misumi, S.: J. Mol. Spect. **46**, 1 (1973)
17. Fuke, K., Nagakura, S.: Bull. Chem. Soc. Jap. **48**, 46 (1975)
18. Fuke, K., Nagakura, S., Kobayashi, T.: Chem. Phys. Letters **31**, 205 (1975)
19. Melzer, G., Schweitzer, D., Hausser, K. H., Colpa, J. P., Haenel, M. W.: Chem. Phys. **39**, 229 (1979)
20. Goldacker, W., Schweitzer, D., Dinse, K. P., Hausser, K. H.: Chem. Phys. **48**, 105 (1980)
21. Kovač, B., Mohraz, M., Heilbronner, E., Boekelheide, V., Hopf, H.: J. Am. Chem. Soc. **102**, 4314 (1980); Kovač, B., Allan, M., Heilbronner, E.: Helv. Chim. Acta **64**, 430 (1981)
22. Gleiter, R., Eckert-Maksić, M., Schäfer, W., Truesdale, E. A.: Chem. Ber. **115**, 2009 (1982)
23. Cram, D. J., Montgomery, C. S., Knox, G. R.: J. Am. Chem. Soc. **88**, 515 (1966); Wolf, A. D., Kane, V. V., Levin, R. H., Jones, M., Jr.: J. Am. Chem. Soc. **95**, 1680 (1973); Kane, V. V., Wolf, A. D., Jones, M., Jr.: J. Am. Chem. Soc. **96**, 2643 (1974); Tobe, Y., Kakiuchi, K., Odaira, Y., Hosaki, T., Kai, Y., Kasai, N.: J. Am. Chem. Soc. **105**, 1376 (1983)
24. Ivanova, T. V., Mokeeva, G., Sveshnikov, B.: Opt. i Spektroskopiya **12**, 586 (1962); Opt. Spectry. **12**, 325 (1962)
25. Azumi, T., McGlynn, S. P.: J. Chem. Phys. **41**, 3131 (1964); **42**, 1675 (1965)
26. Ingraham, L. L.: J. Chem. Phys. **18**, 988 (1950)
27. Koutecký, J., Paldus, J.: Collect. Czech. Chem. Commun. **27**, 599 (1962); Tetrahedron **19**, 2, 201 (1963); Theoret. Chim. Acta (Berl.) **1**, 268 (1963); in: Modern Quantum Chemistry (Istanbul Lectures), Sinanoğlu, O., ed., Part III, p. 229. New York: Academic Press 1965; Paldus, J.: Collect. Czech. Chem. Commun. **28**, 1110, 2667 (1963)
28. Azumi, T., Armstrong, A. T., McGlynn, S. P.: J. Chem. Phys. **41**, 3839 (1964); McGlynn, S. P., Armstrong, A. T., Azumi, T., in: Modern Quantum Chemistry (Istanbul Lectures), Sinanoğlu, O., ed., Part III, p. 203. New York: Academic Press 1965
29. Murrell, J. N., Tanaka, J.: Mol. Phys. **4**, 363 (1964)
30. Vala, M. T., Jr., Hillier, I. H., Rice, S. A., Jortner, J.: J. Chem. Phys. **44**, 23 (1966); Hillier, I. H., Glass, L., Rice, S. A.: J. Chem. Phys. **45**, 3015 (1966); J. Am. Chem. Soc. **88**, 5063 (1966); Hillier, I. H., Rice, S. A.: J. Chem. Phys. **45**, 4639 (1966)
31. Gleiter, R.: Tetrahedron Letters 4453 (1969)
32. Vogler, H., Ege, G., Staab, H. A.: Tetrahedron **31**, 2441 (1975); Mol. Phys. **33**, 923 (1977)
33. Duke, C. B., Lipari, N. O., Salaneck, W. R., Schein, L. B.: J. Chem. Phys. **63**, 1758 (1975)
34. Colpa, J. P., Hausser, K. H., Schweitzer, D.: Chem. Phys. **29**, 187 (1978)
35. Czuchajowski, L., Pietrzycki, W.: J. Mol. Struct. **47**, 423 (1978)
36. Vogler, H.: Theoret. Chim. Acta (Berl.) **60**, 65 (1981)
37. Hanson, A. W.: Acta Cryst. **B33**, 2003 (1977); Hanson, A. W., Cameron, T. S.: J. Chem. Res. (S) 336 (1980); (M) 4201 (1980); Irngartinger, H., Hekeler, J., Lang, B. M.: Chem. Ber. **116**, 527 (1983)

38. Pariser, R., Parr, R. G.: J. Chem. Phys. **21**, 466, 767, (1953); Pople, J. A.: Trans. Faraday Soc. **49**, 1375 (1953); Proc. Phys. Soc. London **A68**, 81 (1955)
39. Mataga, N., Nishimoto, K.: Z. Physik. Chem. (Frankfurt) **12**, 335 (1957); **13**, 140 (1957)
40. Dewar, M. J. S., Klopman, G.: J. Am. Chem. Soc. **89**, 3089 (1967)
41. Dewar, M. J. S., Hojvat (Sabelli), N. L.: J. Chem. Phys. **34**, 1232 (1961); Proc. Roy. Soc. **A264**, 431 (1961); Dewar, M. J. S., Sabelli, N. L.: J. Chem. Phys. **66**, 2310 (1962); Ohno, K.: Theor. Chim. Acta (Berl.) **3**, 219 (1964); Klopman, G.: J. Am. Chem. Soc. **86**, 4550 (1964)
42. Coulson, C. A., Rushbrooke, G. S.: Proc. Camb. phil. Soc. math. phys. Sci. **36**, 193 (1940)
43. Pariser, R.: J. Chem. Phys. **24**, 250 (1956)
44. Koopmans, T. A.: Physica **1**, 104 (1934)
45. Shida, T., Iwata, S.: J. Am. Chem. Soc. **95**, 3473 (1973)
46. Truesdale, E. A., Cram, D. J.: J. Am. Chem. Soc. **95**, 5825 (1973); Trampe, S., Menke, K., Hopf, H.: Chem. Ber. **110**, 371 (1977)
47. Boekelheide, V., Hollins, R. A.: J. Am. Chem. Soc. **95**, 3201 (1973); Hollins, R. A.: Doctoral Dissertation, University of Oregon, 1971
48. Kleinschroth, J., Hopf, H.: Angew. Chem. **91**, 336 (1979); Angew. Chem. Int. Ed. Engl. **18**, 329 (1979)
49. Gilb, W., Menke, K., Hopf, H.: Angew. Chem. **89**, 177 (1977); Angew. Chem. Int. Ed. Engl. **16**, 191 (1977)
50. Gray, R., Boekelheide, V.: Angew. Chem. **87**, 138 (1975); Angew. Chem. Int. Ed. Engl. **14**, 107 (1975)
51. Schirch, P. F. T., Boekelheide, V.: J. Am. Chem. Soc. **101**, 3125 (1979)
52. Sekine, Y., Brown, M., Boekelheide, V.: J. Am. Chem. Soc. **101**, 3126 (1979)
53. Compare f.i. the spectrum of **2**(1,4) with that of its dihydro derivative; Jenny, W., Reiner, J.: Chimia **24**, 69 (1970)
54. Bolovinos, A., Philis, J., Pautos, E., Tsekeris, P., Andritsopoulos, G.: J. Mol. Spect. **94**, 55 (1982)
55. Vergragt, Ph. J., Kooter, J. A., van der Waals, J. H.: Mol. Phys. **33**, 1523 (1977)
56. Spanget-Larsen, J., Haider, R., Gleiter, R.: Helv. Chim. Acta. **66**, 1441 (1983)

Received July 22, 1983